

The Dependence of the EIT Wave Velocity on the Magnetic Field Strength

H.Q. Yang · P.F. Chen

Received: 26 November 2009 / Accepted: 21 June 2010 / Published online: 22 July 2010
© Springer Science+Business Media B.V. 2010

Abstract “EIT waves” are a wavelike phenomenon propagating in the corona, which was initially observed in the extreme ultraviolet (EUV) wavelength by the EUV Imaging Telescope (EIT). Their nature is still elusive, with the debate on-going between fast-mode wave model and non-wave model. In order to distinguish between these models, we investigate the relation between the EIT wave velocity and the local magnetic field in the corona. It is found that the two parameters show significant negative correlation in most of the EIT wave fronts, *i.e.*, the EIT wave propagates more slowly in the regions of stronger magnetic field. Such a result poses a big challenge to the fast-mode wave model, which would predict a strong positive correlation between the two parameters. However, it is demonstrated that such a result can be explained by the fieldline stretching model, *i.e.*, that “EIT waves” are the propagation of apparent brightenings, which are generated by successive stretching of closed magnetic field lines pushed by the erupting flux rope during coronal mass ejections (CMEs).

Keywords Magnetic fields · Sun: activity · Sun: corona · Waves

1. Introduction

EIT waves were discovered by the EUV Imaging Telescope (EIT) (Delaboudinière *et al.*, 1995) aboard the Solar and Heliospheric Observatory (SOHO) initially in the 195 Å channel (Moses *et al.*, 1997; Thompson *et al.*, 1999). They are transient wavelike disturbances that propagate almost over the solar disk and are followed by expanding dimmings (Thompson *et al.*, 1998, 1999). Later, they were also identified in other channels like 171 Å, 284 Å, and 304 Å (Wills-Davey and Thompson, 1999; Zhukov and Auchère, 2004;

H.Q. Yang · P.F. Chen
Department of Astronomy, Nanjing University, Nanjing 210093, China

P.F. Chen (✉)
Key Laboratory of Modern Astronomy and Astrophysics (Nanjing University), Ministry of Education,
Nanjing, China
e-mail: chenpf@nju.edu.cn

Long *et al.*, 2008). They originate around a flare site and propagate outward, avoiding strong magnetic features and neutral lines and stopping near coronal holes (Thompson *et al.*, 1999) or near the magnetic separatrix between active regions (Delannée and Aulanier, 1999). The intriguing phenomenon provoked a lot of controversies on the driving source and its nature (*e.g.*, Delannée, 2000; Chen, 2008). It is now becoming widely accepted that EIT waves are physically associated with CMEs, rather than solar flares (Biesecker *et al.*, 2002; Cliver *et al.*, 2005; Chen, 2006). Especially, Chen (2009a) and Dai *et al.* (2010) found that EIT wave fronts are cospatial with CME frontal loops.

The debate on the nature of EIT waves has been continuing for more than ten years. EIT waves were initially explained as the counterparts of chromospheric Moreton waves (Thompson *et al.*, 1999). Moreton waves are propagating fronts visible mainly in the H α line wings, traveling with a velocity of 500–2000 km s⁻¹ (Moreton and Ramsey, 1960). They were successfully explained to be due to coronal fast-mode waves sweeping the chromosphere (*see, e.g.*, Uchida, 1968). Following this line of thought, Wang (2000) and Wu *et al.* (2001) numerically compared the propagation of fast-mode waves with the EIT wave observations, and they claimed that the trajectory of the fast-mode wave front matches the EIT wave very well. The cospatiality of a sharp front in the EIT image with the H α Moreton wave front in the 24 September 1997 event reinforced such a conjecture (Thompson *et al.*, 2000). However, there is dispute about the relation between this sharp EIT wave front and the ensuing diffuse EIT wave fronts. Some authors, *e.g.*, Warmuth, Mann, and Aurass (2005), propose that the sharp front evolves to the diffuse fronts, whereas others, *e.g.*, Chen, Fang, and Shibata (2005), suggest that they are of different origin, with the sharp front being a real coronal Moreton wave, and the ensuing diffuse fronts being the so-called EIT wave in the general sense. In their model, the sharp front moved out of the solar disk and was not visible in the ensuing EIT images, since the cadence of SOHO/EIT, ≈ 15 min, is too long.

The fast-mode wave model for EIT waves was first questioned by Delannée and Aulanier (1999), who proposed that EIT waves should be related to the magnetic reconfiguration. Based on MHD numerical simulations, Chen *et al.* (2002) proposed that EIT waves are apparently moving brightenings which are generated by the successive stretching of the closed field lines, being pushed by the erupting flux rope. The theory can explain the following observational features:

- i*) The EIT wave velocity is typically three times slower than fast-mode wave velocity.
- ii*) A substantial outflow is present in the dimming region and absent in the EIT wave front (Harra and Sterling, 2003).
- iii*) The EIT wave velocity is uncorrelated with the velocity of type II radio bursts (Klassen *et al.*, 2000).

The model is also consistent with statistical studies which show that EIT waves are more closely associated with CME than solar flares (Biesecker *et al.*, 2002; Chen, 2006). Besides, some authors proposed alternative models in terms of slow-mode waves (Wills-Davey, DeForest, and Stenflo, 2007; Wang, Shen, and Lin, 2009) or successive reconnection (Attrill *et al.*, 2007).

According to the fast-wave model, one would expect to see a strong positive correlation between EIT wave velocity and the local fast-mode wave velocity or the local magnetic field strength. However, in the fieldline stretching model of Chen *et al.* (2002, 2005), the EIT wave velocity is determined by both magnetic field strength and magnetic configuration (Chen, 2009b), *e.g.*, a highly stretched configuration leads to a small EIT wave velocity. Therefore, one would not see a significant positive correlation between EIT wave velocity and the local fast-mode wave velocity or the field strength. In particular, Chen (2009b)

showed in an assumed magnetic configuration that, as the EIT wave propagates outward just across the boundary of the source active region, the fast-mode wave velocity decreases with distance, whereas the EIT wave velocity increases. The generality of this feature awaits further investigation. However, it implies that it is easy to distinguish the fast-wave model and the fieldline stretching model by studying the correlation between EIT wave velocities and the local magnetic field strength, which is the aim of this paper. Observations and the data analysis are described in Section 2; the results are presented in Section 3, and discussions are given in Section 4.

2. Observations and Data Analysis

The two EIT wave events studied in this paper took place on 19 May 2007 and 7 December 2007. Both were located near the solar disk center in the field of view of the Extreme Ultra Violet Imager (EUVI) (Howard *et al.*, 2008) on board the Solar Terrestrial Relations Observatory Ahead (STEREO A) satellite, which allows for a precise measurement of the EIT wave velocity.

There are four channels in STEREO/EUVI observations, *i.e.*, 171 Å (the formation temperature $T \approx 1$ MK), 195 Å ($T \approx 1.5$ MK), 284 Å ($T \approx 2$ MK), and 304 Å. It is noted that the 304 Å channel has a coronal contribution from the Si XI line ($T \approx 1.6$ MK), in addition to the chromospheric line He II ($T \approx 80\,000$ K) (Brosius *et al.*, 1996; Long *et al.*, 2008). Although EIT waves are more evident in 195 Å than 171 Å (Wills-Davey and Thompson, 1999), we use the 171 Å images to derive the EIT wave propagation velocities, since the time cadence (≈ 2.5 min) is much better than that of the 195 Å channel (≈ 10 min).

In order to derive the strength of the coronal magnetic field, we use the potential field extrapolated from the synoptic magnetogram of Michelson Doppler Imager (MDI) telescope (Scherrer *et al.*, 1995) on board the SOHO satellite with the potential field source surface (PFSS) technique (Schrijver and Derosa, 2003). Since EIT wave fronts are significantly bright in the low corona (*e.g.*, Cohen *et al.*, 2009), the magnetic field is taken at the height of $0.06R_{\odot}$ in the extrapolated potential field.

Since the STEREO/EUVI and SOHO/MDI observe the Sun at different times and directions, an important step is to coalign these two data sets. For that purpose, both data sets are coaligned with SOHO/EIT images, since EUVI and EIT use the same emission lines, while MDI and EIT are both aboard the SOHO satellite. First, we derotate and remap the images of EUVI to that of EIT. As an example, the two panels of Figure 1 display the corrected 171 Å images from SOHO/EIT (left) and STEREO/EUVI (right) at 15:24:00 UT on 18 May 2007. The correlation coefficient of the two images is 0.96. After being remapped to the Earth view, running difference images of STEREO/EUVI are taken to show the propagation of EIT waves. As an example, Figure 2 depicts the evolution of the EIT wave event on 19 May 2007. Second, the distribution of the radial component of the magnetic field (B_r) at the height of $0.06R_{\odot}$ is taken from the extrapolated coronal field, and it is derotated and remapped to the same time as the EUVI images. Figure 3 shows the corresponding B_r distribution for the two EIT wave events. Note that B_r is the main component of the magnetic field outside active regions.

3. Results

From the running difference images as shown in Figure 2, we can manually trace the location of the EIT wave front at each time, which is illustrated in Figure 4 as solid lines. As the EIT

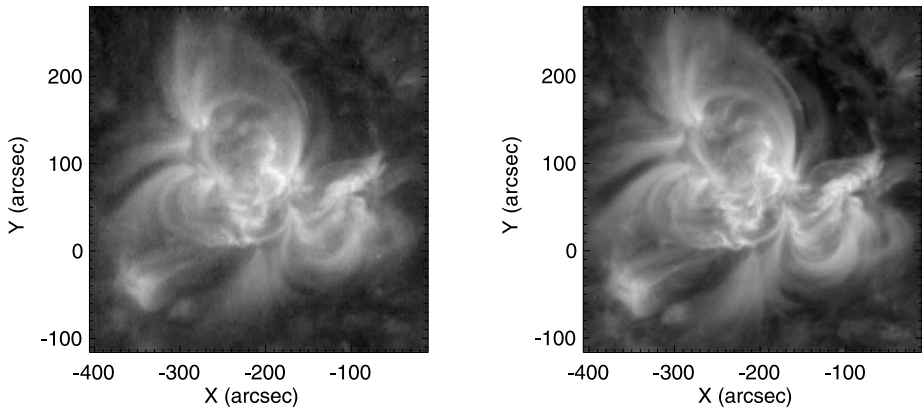
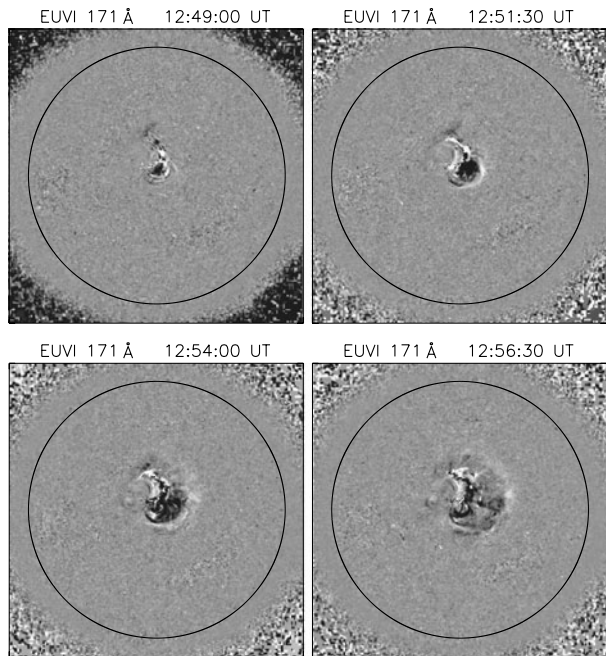


Figure 1 The image of SOHO/EIT (left) and the corrected image of STEREO/EUVI (right) at 15:24:00 UT on 19 May 2007 in the bandpass 171 Å. The correlation coefficient of the two images is 0.96.

Figure 2 The base difference images of the EIT wave event at four times from 12:49:00 UT to 12:56:30 UT on 19 May 2007 observed by STEREO/EUVI showing the wave propagation and the dimming regions on the solar disk. The black circles mark the solar limb. The time of the base image is 12:46:30 UT.



wave front appears diffuse with time and the magnetic field becomes weak far away from the active region, we measure the EIT wave propagation close to the active region only. The left panel displays the propagation of the EIT waves at six times from 12:46:30 UT to 12:59:00 UT for the 19 May 2007 event, and the right panel displays the propagation of the EIT waves at six times from 04:28:30 UT to 04:41:00 UT for the 7 December 2007 event. Note that only the evident portion of each EIT wave front is traced, so that the first event is traced mainly in the west hemisphere, whereas the second event in the east hemisphere.

In order to derive the propagation velocity, we select 20 starting points along the first visible EIT wave front, and then track their trajectories with the Huygens plotting technique as

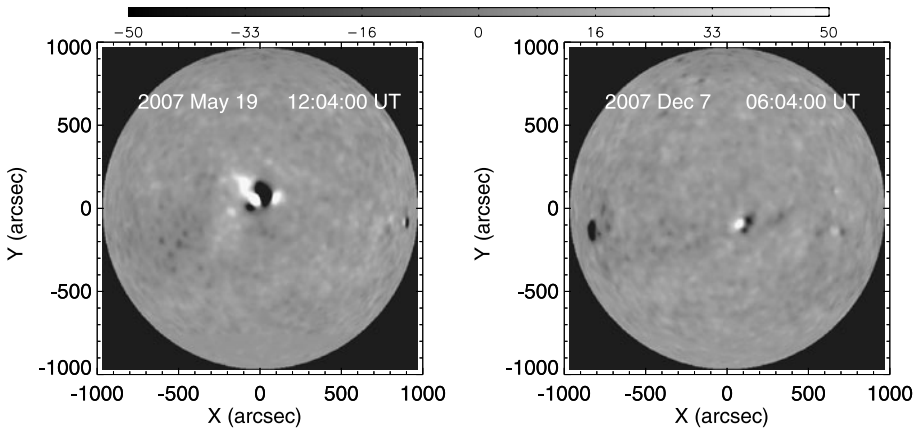


Figure 3 The corrected full disk distributions of the radial component of magnetic field (B_r) at the height of $0.06R_\odot$ for the two EIT events, which are extrapolated from the MDI magnetogram on the solar surface.

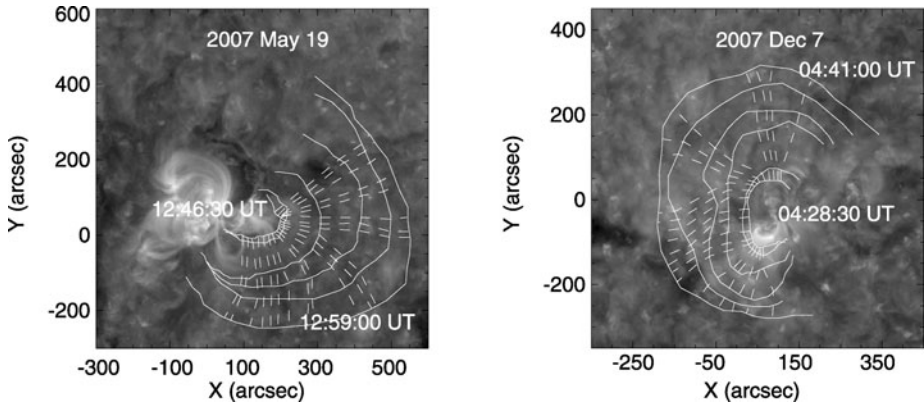


Figure 4 Huygens plotting of the EIT wave front propagation in the 19 May 2007 event (left) and the 7 December 2007 event (right) in the bandpass of 171 \AA . The solid lines correspond to the wave fronts at different times, while the dashed lines show the propagating trajectories.

done in Wills-Davey and Thompson (1999) and Zhukov, Rodriguez, and de Patoul (2009). The trajectories are displayed as dashed lines in Figure 4. The velocity is obtained by the three-point central difference scheme. Therefore, for each trajectory, velocities at four times can be obtained. The error in the wave front position is estimated to be ± 2 pixels, following Zhukov, Rodriguez, and de Patoul (2009). The local magnetic field at each position is determined by averaging the surrounding 3×3 pixels in the extrapolated coronal field at the height of $0.06R_\odot$ above the solar surface.

The scatter plot of the EIT wave velocity (V_{EIT}) vs. the radial component of the magnetic field (B_r) for the 19 May 2007 event is displayed in Figure 5, where four panels correspond to wave fronts at 12:49:00 UT, 12:51:30 UT, 12:54:00 UT, and 12:56:30 UT. It is seen that only at 12:49:00 UT, a very weak positive correlation exists between V_{EIT} and B_r (upper left panel), where V_{EIT} increases slightly as B_r increases by more than 10 times. In the ensuing

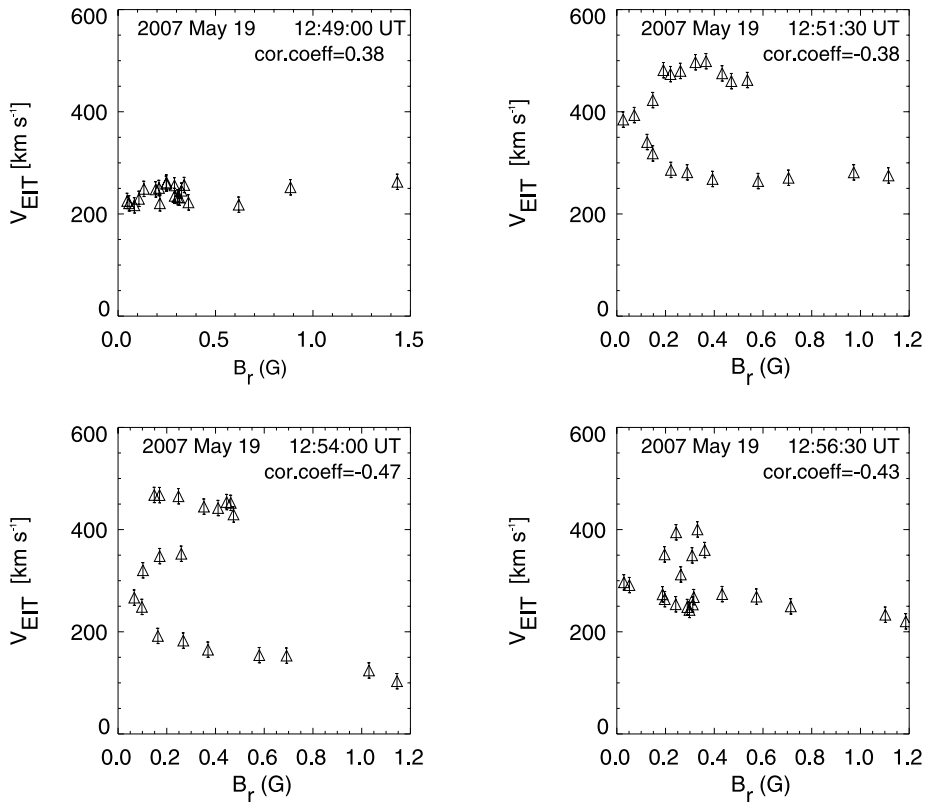


Figure 5 The relation between EIT wave velocity and magnetic field strength for the 19 May 2007 event. The four panels correspond to 12:49:00 UT, 12:51:30 UT, 12:54:00 UT, 12:56:30 UT, respectively.

times, however, V_{EIT} and B_r present a negative correlation, where EIT waves tend to move more slowly at the site with a stronger magnetic field.

The scatter plot of V_{EIT} vs. B_r for the 7 December 2007 event is displayed in Figure 6, where 4 panels correspond to the EIT wave fronts at 04:28:30 UT, 04:31:00 UT, 04:33:30 UT, and 04:36:00 UT, respectively. All these panels reveal that V_{EIT} is negatively correlated to B_r , with the correlation coefficient being smaller than -0.7 at three times.

4. Discussion

“EIT waves” are often explained in terms of fast-mode magnetoacoustic waves in the corona (see, *e.g.*, Wang, 2000; Wu *et al.*, 2001; Vršnak *et al.*, 2002; Warmuth *et al.*, 2004; Grechnev *et al.*, 2008; Pomoell, Vainio, and Kissmann, 2008; Gopalswamy *et al.*, 2009; Patsourakos *et al.*, 2009). However, the wave model cannot explain the following features of “EIT waves”: see Wills-Davey, DeForest, and Stenflo (2007) and Chen (2008), for details.

- i) The “EIT wave” velocity is significantly smaller than those of Moreton waves; the latter are well established to be due to fast-mode waves in the corona.
- ii) The “EIT wave” velocities have no correlation with those of type II radio bursts (Klassen *et al.*, 2000).

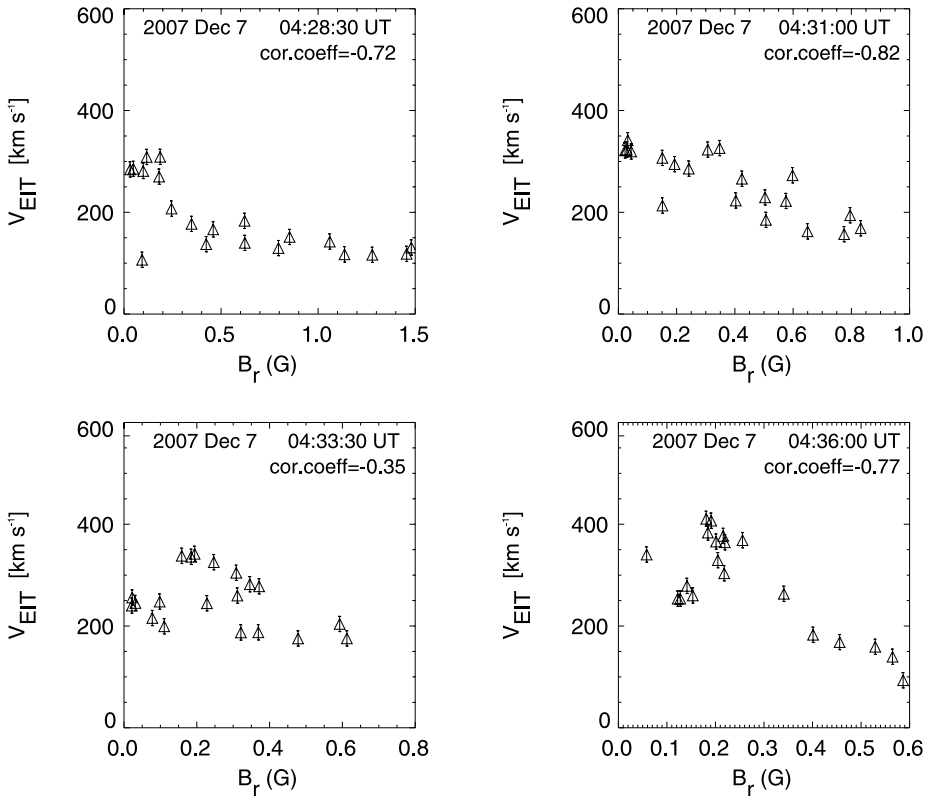
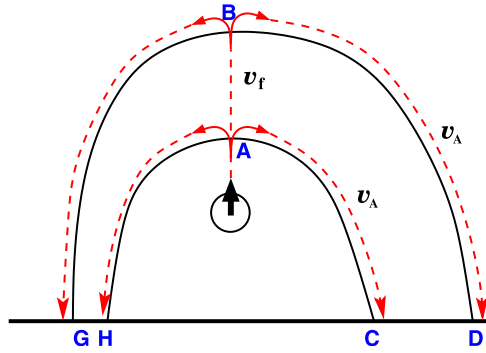


Figure 6 The relation between the EIT wave velocity and the magnetic field strength for the 7 December 2007 event. The four panels correspond to 04:28:30 UT, 04:31:00 UT, 04:33:30 UT, 04:36:00 UT, respectively.

- iii) The “EIT wave” fronts may stop when they meet with magnetic separatrices (Delannée and Aulanier, 1999).
- iv) The “EIT wave” velocity may be below 100 km s^{-1} (see, e.g., Long *et al.*, 2008), which is even smaller than the sound speed in the corona. Moreover, the rotation of EIT wave fronts reported by Podladchikova and Berghmans (2005) was found to be linked to the filament rotation, implying that EIT waves might not be fast-mode waves (Attrill *et al.*, 2007). Note that it may be argued that the lack of correlation between the velocities of EIT waves and type II radio bursts is due to that the former are located at the leg, while the latter are at the top of the same fast-mode wave. However, the velocities of Moreton waves and type II radio bursts do show a linear correlation (Pinter, 1977), although the Moreton wave is also located at the leg of the type II radio burst-related shock wave.

In order to distinguish whether EIT waves are fast-mode waves or not, we investigated the relation between the EIT wave velocity and the local magnetic field with the high-cadence observations from STEREO/EUVI. With the Huygens plotting technique, the distribution of the EIT wave velocity along each front at four times from two EIT wave events was derived. It is found that except at one moment, when the EIT wave velocity (V_{EIT}) is slightly positively correlated with the local magnetic field (B_r), V_{EIT} at all other moments is negatively correlated with B_r , and at some moments, the negative correlation is rather significant. In

Figure 7 Sketch of the fieldline stretching model for EIT waves proposed by Chen *et al.* (2002, 2005), where solid lines are the magnetic field, and dashed lines indicate how the magnetic fieldline stretching is transferred with the local fast-mode wave speed, *i.e.*, the Alfvén speed V_A along the field line and $V_f = \sqrt{V_A^2 + V_s^2}$ perpendicular to the field line, where V_s is the sound speed.



order to examine the validity of the result, we also calculated the relation between V_{EIT} and B_r , with B_r being taken at heights like $0.3R_\odot$ and $0.1R_\odot$. It is found that the result does not change. Such a result poses a big challenge to the fast-mode wave model for EIT waves, since the model would predict a strong positive correlation between V_{EIT} and B_r .

It would then be interesting to check whether the significant negative correlation between V_{EIT} and B_r can be explained by the fieldline stretching model proposed by Chen *et al.* (2002, 2005). The fieldline stretching model is illustrated in Figure 7: as the flux rope is ejected upward, all the overlying field lines will be pushed to stretch up, and for each fieldline, the stretching starts from the top part. That is to say, the perturbation propagates from point A to C with fast-mode wave speed, by which the EIT wave front reaches point C. Note that the fast-mode wave speed along the magnetic field line is equal to the Alfvén speed V_A . Then the perturbation propagates from point A to B and next to D with the local fast-mode wave speed $V_f = \sqrt{V_A^2 + V_s^2}$ (here V_s is the sound speed), by which a second front reaches point D. The apparent velocity of the EIT wave is the distance CD divided by the time difference of the perturbation transfer, *i.e.*,

$$V_{EIT} = CD/\Delta t, \tag{1}$$

where $\Delta t = \int_A^B 1/V_f ds + \int_B^D 1/V_A ds - \int_A^C 1/V_A ds$. According to this model, we can calculate the EIT wave velocity profile for any magnetic configuration.

In order to get an asymmetric magnetic configuration, we put an oblique magnetic dipole below the solar surface, with a line current (along the z -direction) at $x = -2.4$ and $y = -5.5$, and another line current (along the negative z -direction) at $x = -2.6$ and $y = -5.7$. The magnetic field is plotted in the left panel of Figure 8, with the typical magnetic field being ≈ 3.3 gauss. From the figure we can see that the magnetic field left to the magnetic neutral line is stronger than that to the right. For simplicity, we assume a uniform and isothermal pure hydrogen plasma with the electron number density of 10^8 cm^{-3} and temperature of 10^6 K . The resulting typical Alfvén speed is $V_{A0} = 720 \text{ km s}^{-1}$. The corresponding EIT wave velocity profile, which is calculated from Equation (1), is depicted in the right panel of Figure 8, where the wave velocity is in units of V_{A0} . It is seen that the EIT wave velocity profile is complicated. Within $|x| \leq 2$, the EIT wave velocity (V_{EIT}) is higher on the left side, whereas as $|x|$ is larger than two, V_{EIT} becomes higher on the right side. This means that for the magnetic field in the left panel of Figure 8, V_{EIT} and B_r are correlated positively near the neutral line and negatively further out. Such a result is qualitatively consistent with the observed features presented in Section 3.

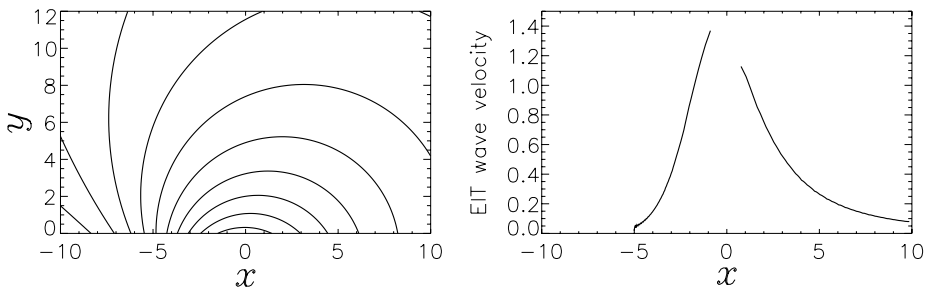


Figure 8 Left: an asymmetric magnetic configuration corresponding to an oblique magnetic dipole below the solar surface; right: the corresponding EIT wave velocity distribution along the horizontal distance. The velocity is in units of 720 km s^{-1} .

By comparing the top two panels in either Figures 5 or 6, it can also be seen that both events analyzed in this paper show that the EIT wave velocity increases as the front propagates outward near the boundary of the source active region. This confirms the result presented in Long *et al.* (2008). Chen (2009b) claimed that this feature poses another big challenge for the fast-mode wave model for EIT waves, which implies a reduction of EIT wave velocity away from the active region since the fast-mode wave speed is much larger near the active region than in the quiet region. Chen (2009b) also demonstrated that the acceleration can be well accounted for in the fieldline stretching model. The reason is quite straightforward: according to their model (Chen *et al.*, 2002, 2005), as illustrated in Figure 7, if the magnetic configuration is highly stretched, *i.e.*, the distance between points A and B is larger, the apparent EIT wave velocity derived from Equation (1) would be smaller. The boundary of active regions does present such a kind of stretched magnetic configuration, as demonstrated in Chen (2009b). Such a feature is absent in our Figure 8, since its magnetic field does not decrease significantly from the source active region to the quiet region as in the real case. Veronig, Temmer, and Vršnak (2008) also analyzed the 19 May 2007 event. However, they claimed that the EIT wave velocity decreases with the distance from the source active region as expected from the fast-mode wave model. The discrepancy between their results and ours, as well as in Long *et al.* (2008), is probably due to the fact that they did not show the EIT wave propagation before 12:52:00 UT, when the EIT wave velocity was increasing.

Note that we focused our study on the EIT wave propagation near the source active region, where the significant variation of the EIT wave velocity occurs. In the quiet region far from the source active region, the EIT wave velocity becomes relatively stable (Ma *et al.*, 2009). With a suitable choice of the coronal density model, it would be easier to reproduce the EIT wave propagation in the large scale as done by Wang (2000) and Wu *et al.* (2001), since SOHO/EIT only captured typically three snapshots of an EIT wave. However, it is hard to imagine that the negative correlation between EIT wave velocity and the local magnetic field strength near the boundary of the source active region can be reproduced in the fast-mode wave framework.

To summarize, we analyzed the relation between EIT wave velocity (V_{EIT}) and the local magnetic field (B_r) in two events observed by STEREO/EUVI with a high cadence. It is found that V_{EIT} and B_r are negatively correlated in most of the fronts, except along one front where V_{EIT} and B_r show a weak positive correlation. It is further revealed that such features, which pose a big challenge for the fast-mode wave model for EIT waves, can be well explained by the fieldline stretching model proposed by Chen *et al.* (2002, 2005).

Acknowledgements The research is supported by the Chinese foundations 2006CB806302 and NSFC (10403003, 10933003, and 10673004). We thank the referee for constructive comments that helped to improve the paper and M.L. Derosa for the help on the use of PFSS routine. The SECCHI data used here were produced by an international consortium of USA, UK, Germany, Belgium, and France. SOHO is a project of international cooperation between ESA and NASA.

References

- Attrill, G.D.R., Harra, L.K., van Driel-Gesztelyi, L., Démoulin, P.: 2007, *Astrophys. J. Lett.* **656**, 101.
- Biesecker, D.A., Myers, D.C., Thompson, B.J., Hammer, D.M., Vourlidas, A.: 2002, *Astrophys. J.* **569**, 1009.
- Brosius, J.W., Davila, J.M., Thomas, R.J., Monsignori-Fossi, B.C.: 1996, *Astrophys. J. Suppl.* **106**, 143.
- Chen, P.F.: 2006, *Astrophys. J.* **641**, L153.
- Chen, P.F.: 2008, *J. Astrophys. Astron.* **29**, 179.
- Chen, P.F.: 2009a, *Astrophys. J. Lett.* **698**, 112.
- Chen, P.F.: 2009b, *Sci. China (G)* **52**, 1785.
- Chen, P.F., Fang, C., Shibata, K.: 2005, *Astrophys. J.* **622**, 1202.
- Chen, P.F., Wu, S.T., Shibata, K., Fang, C.: 2002, *Astrophys. J. Lett.* **572**, 99.
- Cliver, E.W., Laurenza, M., Storini, M., Thompson, B.J.: 2005, *Astrophys. J.* **631**, 604.
- Cohen, O., Attrill, G.D.R., Manchester, W.B., Wills-Davey, M.J.: 2009, *Astrophys. J.* **705**, 587.
- Dai, Y., Auchère, F., Vial, J.-C., Tang, Y.H., Zong, W.G.: 2010, *Astrophys. J.* **708**, 913.
- Delaboudinière, J.-P., Artzner, G.E., Brunaud, J., Gabriel, A.H., Hochedez, J.F., Millier, F., et al.: 1995, *Solar Phys.* **162**, 291.
- Delannée, C.: 2000, *Astrophys. J.* **545**, 512.
- Delannée, C., Aulanier, G.: 1999, *Solar Phys.* **190**, 107.
- Gopalswamy, N., Yashiro, S., Temmer, M., Davila, J., Thompson, W.T., Jones, S., McAteer, R.T.J., Wuelser, J.-P., Freeland, S., Howard, R.A.: 2009, *Astrophys. J. Lett.* **691**, 123.
- Grechnev, V.V., Uralov, A.M., Slemzin, V.A., Chertok, I.M., Kuzmenko, I.V., Shibasaki, K.: 2008, *Solar Phys.* **253**, 263.
- Harra, L.K., Sterling, A.C.: 2003, *Astrophys. J.* **587**, 429.
- Howard, R.A., Moses, J.D., Vourlidas, A., Newmark, J.S., Socker, D.G., Plunkett, S.P., et al.: 2008, *Space Sci. Rev.* **136**, 67.
- Klassen, A., Aurass, H., Mann, G., Thompson, B.J.: 2000, *Astron. Astrophys.* **141**, 357.
- Long, M.D., Peter, T., Gallagher, R.T., Mcateer, J., Bloomfield, D.S.: 2008, *Astrophys. J. Lett.* **680**, 81.
- Ma, S., Wills-Davey, M.J., Lin, J., Chen, P.F., Attrill, G.D.R., Chen, H., Zhao, S., Li, Q., Golub, L.: 2009, *Astrophys. J.* **707**, 503.
- Moreton, G.E., Ramsey, H.E.: 1960, *Publ. Astron. Soc. Pacific* **72**, 357.
- Moses, D., Clette, F., Delaboudinière, J.-P., Artzner, G.E., Bougnet, M., Brunaud, J., et al.: 1997, *Solar Phys.* **175**, 571.
- Patsourakos, S., Vourlidas, A., Wang, Y.M., Stenborg, G., Thernisien, A.: 2009, *Solar Phys.* **259**, 49.
- Pinter, S.: 1977, *Special Rep. AFGL-SR-209*, Air Force Geophysics Laboratory, Hanscom Air Force Base, 35.
- Podladchikova, O., Berghmans, D.: 2005, *Solar Phys.* **228**, 265.
- Pomoell, J., Vainio, R., Kissmann, R.: 2008, *Solar Phys.* **253**, 249.
- Scherrer, P.H., Bogart, R.S., Bush, R.I., Hoeksema, J.T., Kosovichev, A.G., Schou, J., et al.: 1995, *Solar Phys.* **162**, 129.
- Schrijver, C.J., Derosa, M.L.: 2003, *Solar Phys.* **212**, 615.
- Thompson, B.J., Plunkett, S.P., Gurman, J.B., Newmark, J.S., St. Cyr, O.C., Michels, D.J.: 1998, *Geophys. Res. Lett.* **25**, 2465.
- Thompson, B.J., Gurman, J.B., Neupert, W.M., Delaboudinière, J.-P., St. Cyr, O.C., Stezelberger, S., Dere, K.P., Howard, R.A., Michels, D.J.: 1999, *Astrophys. J.* **517**, 151.
- Thompson, B.J., Reynolds, B., Aurass, H., Gopalswamy, N., Gurman, J.B., Hudson, H.S., Martin, S.F., St. Cyr, O.C.: 2000, *Solar Phys.* **193**, 161.
- Uchida, Y.: 1968, *Solar Phys.* **39**, 431.
- Veronig, A.M., Temmer, M., Vršnak, B.: 2008, *Astrophys. J. Lett.* **681**, 113.
- Vršnak, B., Warmuth, A., Brajša, R., Hanslmeier, A.: 2002, *Astron. Astrophys.* **394**, 299.
- Wang, Y.M.: 2000, *Astrophys. J. Lett.* **543**, 89.
- Wang, H., Shen, C., Lin, J.: 2009, *Astrophys. J.* **700**, 1716.
- Warmuth, A., Mann, G., Aurass, H.: 2005, *Astrophys. J. Lett.* **626**, 121.
- Warmuth, A., Vršnak, B., Magdalenic, J., Hanslmeier, A., Otruba, W.: 2004, *Astron. Astrophys.* **418**, 1101.
- Wills-Davey, M.J., Thompson, B.J.: 1999, *Solar Phys.* **190**, 467.

Wills-Davey, M.J., DeForest, C.E., Stenflo, J.: 2007, *Astrophys. J.* **644**, 556.

Wu, S.T., Zheng, H., Wang, S., Thompson, B.J., Plunkett, S.P., Zhao, X.P., Dryer, M.: 2001, *J. Geophys. Res.* **106**, 25089.

Zhukov, A.N., Auchère, F.: 2004, *Astron. Astrophys.* **427**, 705.

Zhukov, A.N., Rodriguez, L., de Patoul, J.: 2009, *Solar Phys.* **259**, 73.